

Geophysical Research Letters



RESEARCH LETTER

10.1029/2020GL087808

Key Points:

- Equatorial deep jets can be reproduced based on the intraseasonal momentum flux convergence alone
- In an idealized ocean model, the deep jets nonlinearly generate both mean eastward and westward flow along the equator

Supporting Information:

- Supporting Information S1

Correspondence to:

S. Bastin,
sbastin@geomar.de;
sbastin@posteo.de

Citation:

Bastin, S., Claus, M., Brandt, P., & Greatbatch, R. J. (2020). Equatorial deep jets and their influence on the mean equatorial circulation in an idealized ocean model forced by intraseasonal momentum flux convergence. *Geophysical Research Letters*, 47, e2020GL087808. <https://doi.org/10.1029/2020GL087808>

Received 4 MAR 2020

Accepted 21 APR 2020

Accepted article online 23 APR 2020

Equatorial Deep Jets and Their Influence on the Mean Equatorial Circulation in an Idealized Ocean Model Forced by Intraseasonal Momentum Flux Convergence

Swantje Bastin¹ , Martin Claus^{1,2} , Peter Brandt^{1,2} , and Richard J. Greatbatch^{1,2} 

¹GEOMAR Helmholtz Centre for Ocean Research, Kiel, Germany, ²Faculty of Mathematics and Natural Sciences, Kiel University, Kiel, Germany

Abstract Equatorial deep jets (EDJ) are vertically stacked, downward propagating zonal currents that alternate in direction with depth. In the tropical Atlantic, they have been shown to influence both surface conditions and tracer variability. Despite their importance, the EDJ are absent in most ocean models. Here we show that EDJ can be generated in an idealized ocean model when the model is driven only by the convergence of the meridional flux of intraseasonal zonal momentum diagnosed from a companion model run driven by steady wind forcing, corroborating the recent theory that intraseasonal momentum flux convergence maintains the EDJ. Additionally, the EDJ in our model nonlinearly generate mean zonal currents at intermediate depths that show similarities in structure to the observed circulation in the deep equatorial Atlantic, indicating their importance for simulating the tropical ocean mean state.

Plain Language Summary In the tropical Atlantic Ocean between 500 and 2,000 m depth, a system of ocean currents called *equatorial deep jets* (EDJ) can be found. This current system consists of multiple currents or *jets* stacked on top of each other and flowing along the equator, alternately (in the vertical) to the east and to the west. The entire system of currents moves slowly downward, such that at a fixed depth, the flow direction reverses periodically. The EDJ are suggested to influence the weather at the ocean surface, as well as the transport of substances in the deep ocean, for example, oxygen that is essential for much of oceanic life. Despite this, their driving mechanisms are not yet fully understood, and they are not yet present in most ocean model simulations. We show here an idealized ocean model experiment that strongly supports the recently developed theory that the EDJ draw most of their flow energy from the interaction with oceanic equatorial waves with a period of about a month. We also show that, when the EDJ are included in our simulation, a set of mean ocean currents develops that shows similarities to what has been measured in the deep tropical Atlantic Ocean.

1. Introduction

The tropical oceans are characterized by strong zonal current systems. One example are the equatorial deep jets (EDJ) that were first discovered in the Indian Ocean in the 1970s by Luyten and Swallow (1976). Later, it was found that there are EDJ in all three ocean basins (Firing, 1987; Gouriou et al., 1999; Hayes & Milburn, 1980; Johnson et al., 2002; Johnson & Zhang, 2003; Leetmaa & Spain, 1981). The EDJ take the form of vertically stacked zonal currents along the equator that alternate in direction with depth. Whereas their vertical wavelength is on the order of a few hundred meters, their zonal structure is coherent over scales comparable to the width of the ocean basins (Gouriou et al., 1999; Johnson & Zhang, 2003; Youngs & Johnson, 2015). Their meridional structure is that of equatorially trapped waves with exponential amplitude decay away from the equator, although there has been some debate about the length scale of this decay, which is larger than expected based on inviscid theory (Greatbatch et al., 2012; Johnson & Zhang, 2003). Their vertical scale is thought to be set by the instability, or resonant triad interaction, of intraseasonal waves (Hua et al., 2008) that are, in turn, excited through instabilities in the western boundary currents (d'Orgeville et al., 2007) or in the upper ocean currents (Ascani et al., 2015). Much of the variability at the equator, especially in the Atlantic, is resonant at frequencies corresponding to basin modes (Brandt et al., 2016; Cane & Moore, 1981), which is also true for the EDJ (e.g., Ascani et al., 2015; d'Orgeville et al., 2007;

©2020. The Authors.

This is an open access article under the terms of the Creative Commons Attribution License, which permits use, distribution and reproduction in any medium, provided the original work is properly cited.

Matthießen et al., 2015; Matthießen et al., 2017). The period of the gravest of these resonant basin modes, T_n , is set by the time it takes for a Kelvin wave to propagate across the basin, be reflected as the gravest long Rossby wave and propagate back to the western boundary, that is,

$$T_n = \frac{4L}{c_n}, \quad (1)$$

where L is the width of the basin, n is the vertical normal mode in question, and c_n is the gravity wave phase speed for that vertical normal mode. Because of the dependence on the width of the basin, the EDJ in the Pacific vary on considerably longer time scales than those in the Indian or Atlantic Oceans (Youngs & Johnson, 2015). We will focus on the Atlantic EDJ in this article, where, in observations, the EDJ period is approximately 4.5 years (Bunge et al., 2008; Brandt et al., 2011) and their vertical structure is best described by the 15th baroclinic mode (Brandt et al., 2008).

Observations of the Atlantic EDJ show that their vertical phase propagation is directed downward. Assuming linear wave theory, this implies upward group velocity, that is, upward energy propagation, also shown in a nonlinear model simulation by Matthießen et al. (2015). Consistent with this, variability at the dominant EDJ period has been found in different surface parameters in the eastern equatorial Atlantic region, including the sea surface temperature, winds, rainfall, and geostrophic surface currents (Brandt et al., 2011). Additionally, the EDJ influence oxygen concentrations in the intermediate and deep ocean, both the variability and the mean state (Brandt et al., 2012, 2015). Finally, the EDJ seem to have an influence on the time mean equatorial circulation. Ascani et al. (2015) have shown that there is nonlinear energy transfer between variability at EDJ scales and the mean zonal currents, possibly enhancing the zonal exchange in the equatorial belt. The presence of zonal currents also strengthens the meridional gradients of potential vorticity (Claus et al., 2014), thereby reducing the meridional exchange of momentum, tracers, and particles (Kiko et al., 2017; Ménesguen et al., 2009).

Despite the EDJs' importance for ocean surface variables and deep ocean tracer distribution and variability, their driving mechanisms are not yet completely understood. Claus et al. (2016) showed that, apart from the excitation of the EDJ by barotropic instability of intraseasonal waves, as suggested by Hua et al. (2008), there must also be a mechanism maintaining the EDJ against dissipation directly in their depth range. They argue that given realistic dissipation values, in the absence of forcing, the EDJ energy cannot vertically propagate a much larger distance than the EDJs' vertical wavelength (Claus et al., 2016). A likely mechanism for the EDJ maintenance at depth has recently been proposed by Greatbatch et al. (2018). They showed that there is a positive correlation of the slowly varying zonal velocity associated with the EDJ and the convergence of the meridional flux of intraseasonal zonal momentum. The explanation they propose is that the EDJ deform intraseasonal waves such that the convergence of the intraseasonal momentum flux becomes nonzero and reinforces the deep jets, comparable to the deformation of eddies in the atmospheric jet stream and the accompanying momentum flux convergence.

In this study, we explore the effect of introducing the intraseasonal momentum flux convergence (IMFC) associated with the EDJ, which we diagnose from an idealized, wind-forced model of the tropical Atlantic, as the only momentum forcing into the same model without wind. We can show that it is possible to generate EDJ with realistic amplitude by prescribing the IMFC, corroborating the theory put forward by Greatbatch et al. (2018) that the IMFC likely is the key mechanism responsible for the EDJ maintenance at depth. Additionally we can show that, in our idealized model, the EDJ nonlinearly generate time mean zonal flow in the EDJ depth range, confirming the results of Ascani et al. (2015). The mean zonal circulation that is driven by the EDJ in our model exhibits similarities in structure to the observed mean flow at intermediate depth in the equatorial Atlantic. Section 2 provides a description of the model and our experiment setup. The results are presented in section 3 and summarized and discussed in section 4.

2. Model and Methods

2.1. Model Description and Setup

The results shown in this study have been obtained with an idealized ocean model of the tropical Atlantic basin. We use the Nucleus for European Modelling of the Ocean (NEMO) Version 3.6 (Madec et al., 2017). Our basic setup is inspired by the model setups described in Ascani et al. (2015) and Matthießen et al. (2015).

Our rectangular model basin with closed boundaries extends from 20°S to 20°N and over a width of 55°, mimicking the width of the Atlantic Ocean at the equator. The basin is 5,000 m deep with a flat bottom.

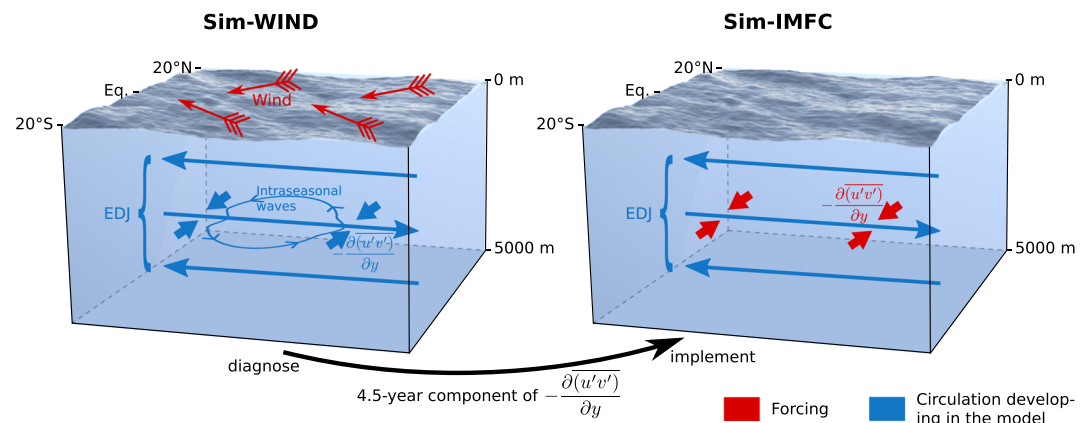


Figure 1. Schematic depiction of the model experiment design.

The horizontal resolution is $0.25^\circ \times 0.25^\circ$, whereas the vertical resolution is, with 200 levels, considerably finer at depth than that usually employed in ocean models to enable the simulation of EDJ. The vertical mixing scheme is Richardson number dependent, following Pacanowski and Philander (1981). We initialize the model with vertical temperature and salinity profiles from the World Ocean Atlas 2018 (Locarnini et al., 2019; Zweng et al., 2019). For more details see the supporting information.

2.2. Experiment Design

We run this idealized model configuration twice (summarized in Figure 1). For the first run, named Sim-WIND in the following, we force the model at the surface with steady, zonally averaged wind stress calculated from NCEP/NCAR reanalysis data (Kalnay et al., 1996; Kistler et al., 2001). With the wind forcing, both intraseasonal waves and EDJ with the same period as found in observations (4.5 years) are present in the model, and the suggested mechanism for maintaining the EDJ through distortion of the intraseasonal waves from Greatbatch et al. (2018) can come into effect (see left panel of Figure 1). From Sim-WIND we diagnose at every grid point in the basin the intraseasonal momentum flux convergence (IMFC) that is associated with the EDJ (i.e., the 4.5-year Fourier component of $-\partial(u'v')/\partial y$, where the overbar/prime denotes variability on time scales larger/smaller than 70 days). The second model run, named Sim-IMFC, is only forced with the diagnosed IMFC; that is, the term is added to the zonal momentum equation at every time step (see right panel of Figure 1). By adding the term to the equation rather than applying a relaxation scheme, we ensure that our forcing does not interfere with other model dynamics.

2.3. Argo Analysis

We use deep velocity data calculated from Argo float measurements by Lebedev et al. (2007), covering a time period of nearly 20 years (2000–2019), for an estimation of the mean zonal flow field at 1,000 m depth in the equatorial Atlantic. The Argo data have been spatially smoothed and corrected for sampling bias associated with the presence of EDJ before taking the time mean, using methods of Edelson and Krolik (1988), Lomb (1976), and Scargle (1982). For details see the supporting information.

3. Results

3.1. Generation of EDJ by Intraseasonal Momentum Flux Convergence

The characteristics of the EDJ that develop in our idealized model simulations can be seen in Figure 2. For a comparison of the modeled EDJ to observations, the reader is referred to the supporting information; here, it is sufficient to say that the main characteristics of the Atlantic EDJ are well represented in our model. The EDJ that emerge through our internal forcing with the intraseasonal momentum flux convergence are very similar to those in the wind-forced simulation, at least between approximately 400 and 1,800 m depth (below that, the diagnosed IMFC is weak, resulting in weak EDJ in Sim-IMFC). The most striking differences between the simulations are the missing near-surface circulation (e.g., the Equatorial Undercurrent) due to the lack of wind forcing, and the strong reduction of variability on frequencies other than the EDJ frequency in Sim-IMFC. Both differences are intended and due to our experiment design (recall, in particular, that Sim-IMFC is forced at a single period of 4.5 years). Figures 2c and 2d show the time series of zonal velocity projected onto the dominant vertical mode. The EDJ in both model simulations have similar amplitudes,

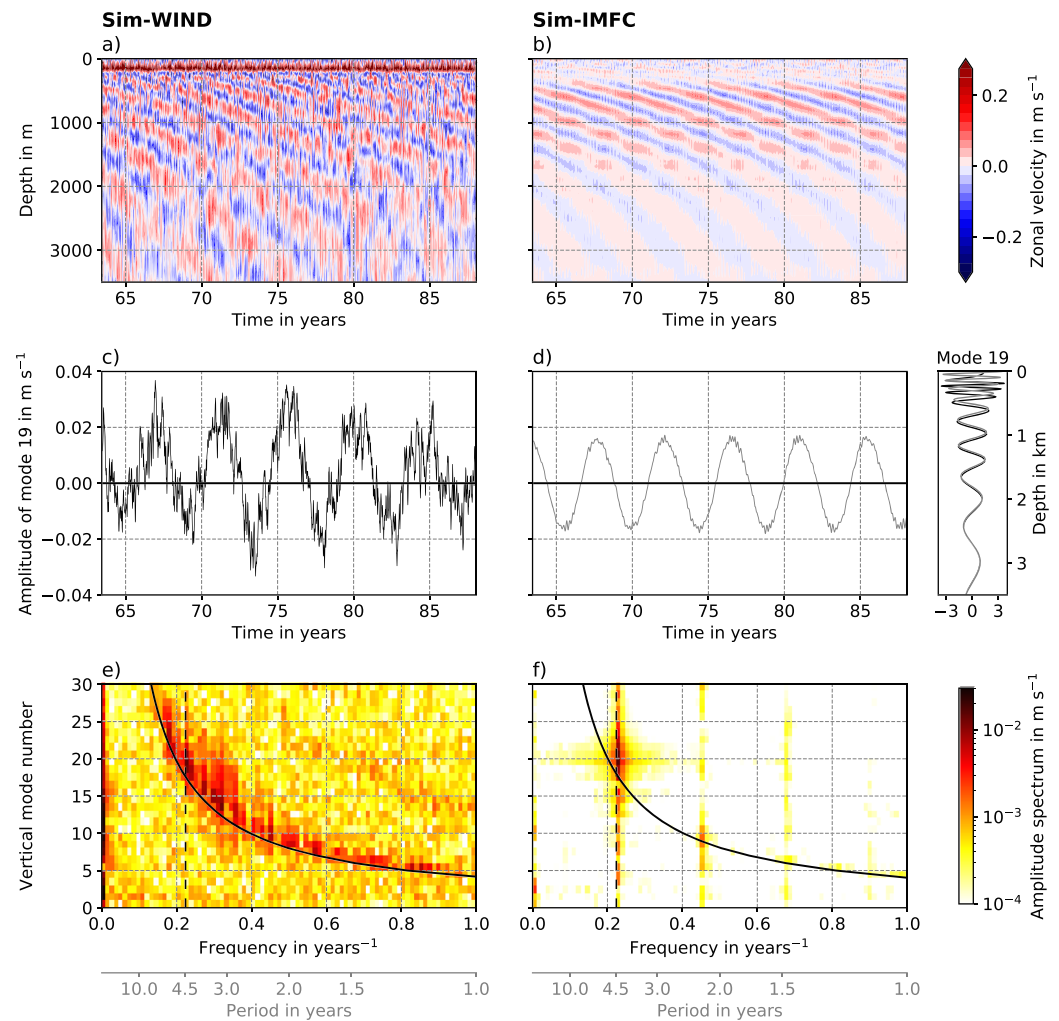


Figure 2. EDJ in the two model runs; Sim-WIND on the left (a, c, and e) and Sim-IMFC on the right (b, d, and f). Panels a and b show Hovmöller diagrams of zonal velocity on the equator in the center of the model basin. Panels c and d show time series of zonal velocity projected onto the 19th vertical normal mode (one of the dominant modes of the EDJ, cf. Panels e and f) at the center of the basin. The associated structure functions from both model runs are shown on the right. Panels e and f show amplitude spectra of zonal velocity at the center of the basin, calculated after the decomposition of the velocity into vertical normal modes. The gravest equatorial basin mode resonance curve is drawn in solid black. The dashed black line indicates the dominant EDJ frequency.

although the amplitude shows more fluctuation in Sim-WIND because of the superposition with variability on different time scales. In Figures 2e and 2f, amplitude spectra of the zonal velocity, projected onto vertical normal modes, at the center of the model basin are shown. The spectral energy is clearly centered around the gravest equatorial basin mode (cf. equation (1) and the solid black line in the figure), and the EDJ (cf. dashed black line) represent a prominent peak.

Although the temporal and vertical (and zonal, not shown) structures of the EDJ in both simulations are similar, the meridional structure is different—in Sim-IMFC, the EDJ are significantly narrower than in Sim-WIND. We attribute the difference in EDJ width to the missing influence of the wind and associated variability in Sim-IMFC and the related changes in effective momentum viscosity (cf. Greatbatch et al., 2012), because it is not connected to the structure of the forcing itself. However, this is a topic that requires further research.

It was already noted by Greatbatch et al. (2018) that the structure and magnitude of the intraseasonal momentum flux convergence agree well with the estimates of Claus et al. (2016) regarding the forcing necessary to maintain the EDJ at depth. This is also true for our simulations: The IMFC varying at the EDJ

frequency that we diagnosed from Sim-WIND has an amplitude of up to $4 \cdot 10^{-9} \text{ m s}^{-2}$ at the equator, which is consistent with both Claus et al. (2016) and Greatbatch et al. (2018). The fact that this IMFC forcing alone can, in our model, drive and maintain EDJ that are realistic in amplitude and structure strongly supports the idea proposed by Greatbatch et al. (2018) based on theoretical considerations that the IMFC is the key process maintaining the EDJ at depth.

3.2. Influence on the Time Mean Zonal Flow

As can be seen from Figure 2f, variability on frequencies different from the forcing frequency is generated nonlinearly in Sim-IMFC. Particularly interesting is the generation of time mean zonal flow from the EDJ variability (at the zero frequency in the spectrum). Figures 3a–3c show the time mean zonal velocity at 1,000 m depth, from both model runs and Argo float data (Lebedev et al., 2007). Note that the color range is scaled by a factor of 5 for Sim-IMFC. In the model, the structure of the mean zonal flow is very similar at all depths where the EDJ are strong, that is, between approximately 400 and 1,800 m. The mean zonal flow at depth in Sim-WIND is dominated by westward flow on the equator and eastward flow approximately 2° north and south of the equator in the western half of the basin. This structure is also found from Argo data in the western basin. The strong westward flow on the equator and the flanking eastward jets at about 2°N/S are usually described as the central part of the equatorial intermediate current system both in the Atlantic and the Pacific Ocean (EICS, cf., e.g., Ascani et al., 2010; Cravatte et al., 2012, 2017; Ménésguen et al., 2019) and have been suggested to originate from dissipation associated with the breaking of downward propagating equatorial Yanai waves by Ascani et al. (2010).

The mean zonal flow that is generated nonlinearly by the EDJ in Sim-IMFC also displays this characteristic structure with one jet on the equator flanked by reversed jets to the north and south: here, however, including a midbasin change of sign that has also been noted by Ascani et al. (2015). In the western part of the basin between 45°W and about 30°W , the generated mean flow is westward on the equator and eastward to the north and south, whereas in the central and eastern parts of the basin between about 25°W and 5°W , there is eastward flow on the equator, flanked by weak westward current bands. The EDJ thus seem to strengthen the equatorial westward and flanking eastward flow that Ascani et al. (2010) attributed to downward propagating Yanai wave beams in the west of the basin but counteract it in the central and eastern basin.

Interestingly, a similar midbasin change of current direction can also be seen in the Argo data. The westward flow on the equator only extends into about one third of the basin and is superseded by eastward flow in some regions close to the center of the basin, resembling the structure of the mean zonal flow generated by the EDJ in Sim-IMFC. This suggests that the Atlantic EDJ play a role in establishing the mean zonal current direction on the equator, in the central basin possibly even reversing the otherwise predominantly westward flow that has so far been considered the central branch of the EICS.

The magnitude of the flow generated by the EDJ in our model only amounts to at most half of the total time mean zonal velocity measured by Argo around the equator in the center of the basin. This is therefore not enough to explain the Argo mean velocity field. However, it is difficult from our idealized model study to infer the exact magnitude of the mean flow that would be generated from the EDJ in the real ocean—for example, the amplitude of the EDJ in our model simulations is rather small (see Figure S5 in the supporting information). Because of the nonlinearity of the time mean zonal flow generation, the real Atlantic EDJ might, with a slightly larger amplitude, generate much stronger mean currents. We have tested the effect of different IMFC forcing amplitudes and thus different EDJ strengths in additional model runs, confirming a larger than linear increase of the mean flow amplitude with linearly increasing EDJ amplitude (shown in the supporting information). The structure of the generated mean flow, however, stays the same for different EDJ amplitudes.

Figures 3d/3e show the dominant terms of the nonlinear energy transfer from the EDJ to the time mean zonal circulation in Sim-IMFC, averaged over different areas around the equator. Consistent with the results of Ascani et al. (2015), the transfer of energy from EDJ to mean zonal flow mainly occurs through the term $-\overline{\partial(u'u')}/\partial x$, whereas some, but less, energy is transferred from the mean flow to the EDJ through $-\overline{\partial(u'v')}/\partial y$ (the overbar denoting the time mean, the prime deviations from the time mean including mainly the EDJ; not to be confused with the IMFC, where the separation of time scales was between intraseasonal and longer than intraseasonal). The energy transfer is largest close to the equator, but the sign is consistent over almost all averaging areas. The fact that $-\overline{\partial(u'u')}/\partial x$ is the responsible term for the energy transfer from

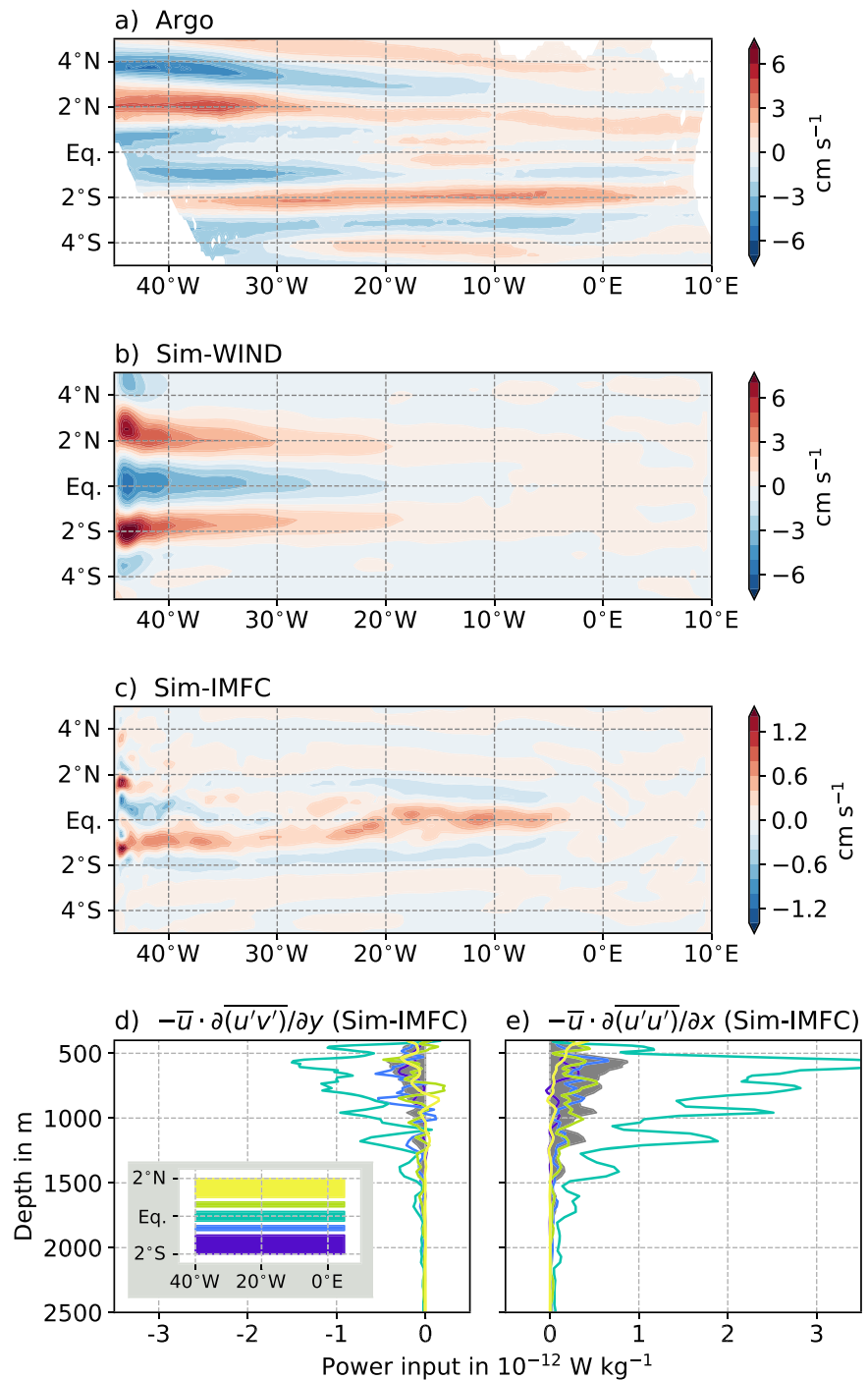


Figure 3. Time mean zonal velocity at 1,000 m depth from Argo (Lebedev et al., 2007, Panel a) and from the model runs (Panels b and c). Panels d and e show the time and space averaged nonlinear power input from EDJ into mean zonal flow from Sim-IMFC. The power input through $-\partial(u'w')/\partial z$ (not shown) is negligible compared to the other two terms. The overline here denotes a time average, whereas the prime denotes all deviations from this time average (i.e., mainly the EDJ). The inset in Panel d shows the averaging areas corresponding to the color-coded curves in Panels d and e; the filled dark gray curve is the average over all five colored areas.

EDJ to mean flow agrees with the zonal structure of the generated mean flow, in particular its midbasin change of direction.

4. Summary and Discussion

In this study, we have shown that it is possible to drive realistic EDJ in an idealized ocean model by forcing only with the convergence of the meridional flux of intraseasonal zonal momentum that is associated with the EDJ in the momentum equation. We have also shown that, in our model, the EDJ nonlinearly generate time mean zonal flow that shows similarities in structure to the mean flow measured by Argo floats at 1,000 m depth along the equator.

The EDJ are stacked zonal jets with large vertical and small zonal wave numbers in the deep equatorial oceans that propagate downward with time, the entire system resembling a resonant equatorial basin mode associated with high vertical baroclinic modes. Apart from their excitation mechanisms that have been the topic of research for some time, one interesting feature of the EDJs' dynamics is the question of how they are maintained against dissipation after their initial generation. Claus et al. (2016) argued that there must be a local forcing process at work in the depth range of the EDJ in order for the EDJ to retain their amplitude over several vertical wavelengths. Greatbatch et al. (2018) suggested that this process could be the deformation of intraseasonal waves by the EDJ, which they argue leads to convergence of the meridional flux of intraseasonal zonal momentum (referred to as intraseasonal momentum flux convergence, IMFC, here), reinforcing the EDJ. As shown by Greatbatch et al. (2018), the magnitude of the IMFC associated with the EDJ agrees well with that of the necessary local forcing amplitude as derived by Claus et al. (2016), making this mechanism a plausible candidate for the EDJ maintenance at depth.

With this study, we were able to confirm the theory proposed by Greatbatch et al. (2018) by showing that the IMFC can actually drive sufficiently strong EDJ in an idealized ocean model. We diagnosed the IMFC varying at the EDJ frequency from a model configuration that is able to simulate EDJ; a rectangular tropical Atlantic basin model driven by steady wind forcing. Applying the diagnosed IMFC as momentum forcing to a companion model without any other forcing (i.e., without wind) yields EDJ that are very similar in their main characteristics to those arising in the wind-forced model, in particular, they reach a similar amplitude. Our results thus strongly corroborate the theory put forward by Greatbatch et al. (2018) that the IMFC is largely responsible for maintaining the EDJ.

One thing to bear in mind concerning our modeling approach is that the generation of the EDJ, in reality, does not happen through IMFC as in our simulation. In the real ocean, the momentum forcing through the IMFC only kicks in when the EDJ are already there and strong enough to distort intraseasonal equatorial waves. How the EDJ are generated in the first place is an ongoing topic of research, but it is generally thought that they originate from a number of different mechanisms that involve instabilities in the upper ocean currents and the deep western boundary currents, which excite deep equatorial intraseasonal variability that rectifies into the EDJ basin modes (e.g., Ascani et al., 2010, 2015; d'Orgeville et al., 2007; Hua et al., 2008; Ménesguen et al., 2019).

Interestingly, in the model configuration that we forced only with IMFC varying at the EDJ frequency, variability also on other time scales appears—in particular there is time mean flow that is generated nonlinearly from the EDJ variability. This has already been shown by Ascani et al. (2015) for specific EDJ basin modes, and indeed, we can show that in our simulation the energy is transferred from EDJ to mean zonal flow mainly through the zonal self-advection of the EDJ, corroborating their results.

The mean zonal flow at intermediate depths that is generated by the EDJ in our model is westward in the western third of the basin, but otherwise predominantly eastward on the equator, in the opposite direction to the mean westward equatorial flow that has been suggested to be driven by downward propagating, dissipating Yanai wave beams (Ascani et al., 2010) and usually thought to be the central part of the system of low-mode, latitudinally alternating zonal jets in the tropical oceans often called the equatorial intermediate current system (EICS, e.g., Ascani et al., 2010; Cravatte et al., 2017; Ménesguen et al., 2019). Indeed, Argo observations from 1,000 m depth in the Atlantic show that on the equator, the mean zonal velocity is clearly westward only in approximately the western third of the basin and becomes eastward in some places around the basin center. Our results thus suggest that the Atlantic EDJ play a role in establishing the mean zonal current direction on the equator. However, this effect might be important only in the equatorial Atlantic

Ocean. In the Pacific, the mean zonal flow at intermediate depth appears to be westward throughout most of the basin (e.g., Cravatte et al., 2017), indicating that here, the influence of the EDJ is not strong enough to reverse the current direction. This is consistent with the fact that the Atlantic EDJ are significantly stronger than those in the Pacific and Indian Oceans (e.g., Youngs & Johnson, 2015). It is also consistent with the much larger basin width, that is, zonal extent of the EDJ, in the Pacific, because the transfer of energy to the mean flow depends on the zonal gradient of EDJ strength, which is likely small over a larger part of the central Pacific compared to the central Atlantic. Eastward flow along the equator as part of the system of latitudinally alternating zonal jets has also been simulated by Qiu et al. (2013) as the result of nonlinear triad interactions of annual baroclinic Rossby waves. However, it should be noted that they used a $1\frac{1}{2}$ -layer reduced-gravity model designed to simulate the off-equatorial zonal jets, not the equatorial circulation. Also, the observed westward equatorial flow in the Pacific suggests that the mechanism that is at work in their model is of minor importance directly on the equator.

It is known that many global biogeochemical ocean models struggle with oxygen and nutrient distributions in the deep tropical oceans. In general, the oxygen minimum zones in the deep eastern ocean basins are larger in models than in reality, likely because the correct ventilation by the equatorial current system is missing (Dietze & Loeptien, 2013; Getzlaff & Dietze, 2013). Associated with this, there is an excess of nutrients in these regions, usually termed “Nutrient Trapping” (Najjar et al., 1992). It has been shown before that the EDJ are responsible for ventilation of the eastern oxygen minimum zones (OMZ), albeit because of the asymmetry in oxygen production and consumption leading to a net eastward oxygen flux due to advection by the EDJ themselves (Brandt et al., 2012). Our results make clear that the Atlantic EDJ likely additionally contribute to OMZ ventilation by generating eastward time mean flow along the equator. The fact that the EDJ are not usually represented in global ocean models thus constitutes a serious shortcoming, and we suggest that including them in ocean models could not only lead to a better representation of the variability, but also of the mean state of the equatorial current system.

Acknowledgments

For more details on model simulations and methods, the reader is referred to the supporting information. Scripts and data necessary to obtain the results presented in this paper can be found online at <https://doi.org/10.5281/zenodo.3689335> (Bastin et al., 2020). NCEP/NCAR reanalysis data were provided by the NOAA/OAR/ESRL PSD, Boulder, Colorado, USA, from their website (at <https://www.esrl.noaa.gov/psd/>). Python was used for analysis, Matplotlib (Hunter, 2007) for plotting. This work has been funded in part by the *Sonderforschungsbereich 754 – Climate-Biogeochemistry Interactions in the Tropical Ocean*. The authors are not aware of financial conflicts/conflicts of interest related to this work. We thank one anonymous reviewer for their helpful comments.

References

- Ascani, F., Firing, E., Dutrieux, P., McCreary, J. P., & Ishida, A. (2010). Deep equatorial ocean circulation induced by a forced-dissipated Yanai beam. *Journal of Physical Oceanography*, 40, 1118–1142. <https://doi.org/10.1175/2010JPO4356.1>
- Ascani, F., Firing, E., McCreary, J. P., Brandt, P., & Greatbatch, R. J. (2015). The deep equatorial ocean circulation in wind-forced numerical solutions. *Journal of Physical Oceanography*, 45, 1709–1734. <https://doi.org/10.1175/JPO-D-14-0171.1>
- Bastin, S., Claus, M., Brandt, P., & Greatbatch, R. J. (2020). Supplementary dataset for Bastin et al. (2020), *Geophysical Research Letters*. (Version 0.1), [data set], Zenodo. <https://doi.org/10.5281/zenodo.3689335>
- Brandt, P., Bange, H. W., Banyte, D., Dengler, M., Didwischus, S.-H., Fischer, T., et al. (2015). On the role of circulation and mixing in the ventilation of oxygen minimum zones with a focus on the eastern tropical North Atlantic. *Biogeosciences*, 12, 489–512. <https://doi.org/10.5194/bg-12-489-2015>
- Brandt, P., Claus, M., Greatbatch, R. J., Kopte, R., Toole, J. M., Johns, W. E., & Böning, C. W. (2016). Annual and semiannual cycle of equatorial Atlantic circulation associated with basin-mode resonance. *Journal of Physical Oceanography*, 46, 3011–3029. <https://doi.org/10.1175/JPO-D-15-0248.1>
- Brandt, P., Funk, A., Hormann, V., Dengler, M., Greatbatch, R. J., & Toole, J. M. (2011). Interannual atmospheric variability forced by the deep equatorial Atlantic Ocean. *Nature*, 473, 497–500. <https://doi.org/10.1038/nature10013>
- Brandt, P., Greatbatch, R. J., Claus, M., Didwischus, S.-H., Hormann, V., Funk, A., et al. (2012). Ventilation of the equatorial Atlantic by the equatorial deep jets. *Journal of Geophysical Research*, 117, C12015. <https://doi.org/10.1029/2012JC008118>
- Brandt, P., Hormann, V., Bourlès, B., Fischer, J., Schott, F. A., Stramma, L., & Dengler, M. (2008). Oxygen tongues and zonal currents in the equatorial Atlantic. *Journal of Geophysical Research*, 113, C04012. <https://doi.org/10.1029/2007JC004435>
- Bunge, L., Provost, C., Hua, B. L., & Kartavtseff, A. (2008). Variability at intermediate depths at the equator in the Atlantic Ocean in 2000–06: Annual cycle, equatorial deep jets, and intraseasonal meridional velocity fluctuations. *Journal of Physical Oceanography*, 38, 1794–1806. <https://doi.org/10.1175/2008JPO3781.1>
- Cane, M. A., & Moore, D. W. (1981). A note on low-frequency equatorial basin modes. *Journal of Physical Oceanography*, 11, 1578–1584. [https://doi.org/10.1175/1520-0485\(1981\)011<1578:ANOLFEI2.0.CO;2](https://doi.org/10.1175/1520-0485(1981)011<1578:ANOLFEI2.0.CO;2)
- Claus, M., Greatbatch, R. J., & Brandt, P. (2014). Influence of the barotropic mean flow on the width and the structure of the Atlantic equatorial deep jets. *Journal of Physical Oceanography*, 44, 2485–2497. <https://doi.org/10.1175/JPO-D-14-0056.1>
- Claus, M., Greatbatch, R. J., Brandt, P., & Toole, J. M. (2016). Forcing of the Atlantic equatorial deep jets derived from observations. *Journal of Physical Oceanography*, 46, 3549–3562. <https://doi.org/10.1175/JPO-D-16-0140.1>
- Cravatte, S., Kessler, W. S., & Marin, F. (2012). Intermediate zonal jets in the Tropical Pacific Ocean observed by argo floats. *Journal of Physical Oceanography*, 42, 1475–1485. <https://doi.org/10.1175/JPO-D-11-0206.1>
- Cravatte, S., Kestenare, E., Marin, F., Dutrieux, P., & Firing, E. (2017). Subthermocline and intermediate zonal currents in the Tropical Pacific Ocean: Paths and vertical structure. *Journal of Physical Oceanography*, 47, 2305–2324. <https://doi.org/10.1175/JPO-D-17-0043.1>
- d’Orgeville, M., Hua, B. L., & Sasaki, H. (2007). Equatorial deep jets triggered by a large vertical scale variability within the western boundary layer. *Journal of Marine Research*, 65, 1–25. <https://doi.org/10.1357/002224007780388720>
- Dietze, H., & Loeptien, U. (2013). Revisiting “nutrient trapping” in global coupled biogeochemical ocean circulation models. *Global Biogeochemical Cycles*, 27, 265–284. <https://doi.org/10.1002/gbc.20029>
- Edelson, R. A., & Krolik, J. H. (1988). The discrete correlation function: A new method for analyzing unevenly sampled variability data. *The Astrophysical Journal*, 333, 646–659. <https://doi.org/10.1086/166773>

- Firing, E. (1987). Deep zonal currents in the central equatorial Pacific. *Journal of Marine Research*, 45, 791–812. <https://doi.org/10.1357/00224087788327163>
- Getzlaff, J., & Dietze, H. (2013). Effects of increased isopycnal diffusivity mimicking the unresolved equatorial intermediate current system in an Earth system climate model. *Geophysical Research Letters*, 40, 2166–2170. <https://doi.org/10.1002/grl.50419>
- Gouriou, Y., Bourlès, B., Mercier, H., & Chuchla, R. (1999). Deep jets in the equatorial Atlantic Ocean. *Journal of Geophysical Research*, 104, 21,217–21,226. <https://doi.org/10.1029/1999JC900057>
- Greatbatch, R. J., Brandt, P., Claus, M., Didwischus, S.-H., & Fu, Y. (2012). On the width of the equatorial deep jets. *Journal of Physical Oceanography*, 42, 1729–1740. <https://doi.org/10.1175/JPO-D-11-0238.1>
- Greatbatch, R. J., Claus, M., Brandt, P., Matthießen, J.-D., Tuchen, F. P., Ascani, F., et al. (2018). Evidence for the maintenance of slowly varying equatorial currents by intraseasonal variability. *Geophysical Research Letters*, 45, 1923–1929. <https://doi.org/10.1002/2017GL076662>
- Hayes, S. P., & Milburn, H. B. (1980). On the vertical structure of velocity in the eastern equatorial Pacific. *Journal of Physical Oceanography*, 10, 633–635. [https://doi.org/10.1175/1520-0485\(1980\)010<0633:OTVSOVi2.0.CO;2](https://doi.org/10.1175/1520-0485(1980)010<0633:OTVSOVi2.0.CO;2)
- Hua, B. L., d'Orgeville, M., Fruman, M. D., Ménesguen, C., Schopp, R., Klein, P., & Sasaki, H. (2008). Destabilization of mixed Rossby gravity waves and the formation of equatorial zonal jets. *Journal of Fluid Mechanics*, 610, 311–341. <https://doi.org/10.1017/S0022112008002656>
- Hunter, J. D. (2007). Matplotlib: A 2D graphics environment. *Computing in Science & Engineering*, 9(3), 90–95. <https://doi.org/10.1109/MCSE.2007.55>
- Johnson, G. C., Kunze, E., McTaggart, K. E., & Moore, D. W. (2002). Temporal and spatial structure of the equatorial deep jets in the Pacific Ocean. *Journal of Physical Oceanography*, 32, 3396–3407. [https://doi.org/10.1175/1520-0485\(2002\)032<3396:TASSOT>2.0.CO;2](https://doi.org/10.1175/1520-0485(2002)032<3396:TASSOT>2.0.CO;2)
- Johnson, G. C., & Zhang, D. (2003). Structure of the Atlantic Ocean equatorial deep jets. *Journal of Physical Oceanography*, 33, 600–609. [https://doi.org/10.1175/1520-0485\(2003\)033<0600:SOTAOE>2.0.CO;2](https://doi.org/10.1175/1520-0485(2003)033<0600:SOTAOE>2.0.CO;2)
- Kalnay, E., Kanamitsu, M., Kistler, R., Collins, W., Deaven, D., Gandin, L., et al. (1996). The NCEP/NCAR 40-year reanalysis project. *Bulletin of the American Meteorological Society*, 77, 437–471. [https://doi.org/10.1175/1520-0477\(1996\)077<0437:TNYRP>2.0.CO;2](https://doi.org/10.1175/1520-0477(1996)077<0437:TNYRP>2.0.CO;2)
- Kiko, R., Biastoch, A., Brandt, P., Cravatte, S., Hauss, H., Hummels, R., et al. (2017). Biological and physical influences on marine snowfall at the equator. *Nature Geoscience*, 10, 852–858. <https://doi.org/10.1038/NGEO3042>
- Kistler, R., Kalnay, E., Collins, W., Saha, S., White, G., Woollen, J., et al. (2001). The NCEP/NCAR 50-year reanalysis: Monthly means CD-ROM and documentation. *Bulletin of the American Meteorological Society*, 82, 247–268. [https://doi.org/10.1175/1520-0477\(2001\)082<0247:TNNYRM>2.3.CO;2](https://doi.org/10.1175/1520-0477(2001)082<0247:TNNYRM>2.3.CO;2)
- Lebedev, K. V., Yoshinari, H., Maximenko, N. A., & Hacker, P. W. (2007). YoMaHa'07: Velocity data assessed from trajectories of Argo floats at parking level and at the sea surface (IPRC Technical Note No. 4(2) 16 p). updated as of November 2019.
- Leetmaa, A., & Spain, P. F. (1981). Results from a velocity transect along the equator from 125° to 159° W. *Journal of Physical Oceanography*, 11, 1030–1033. [https://doi.org/10.1175/1520-0485\(1981\)011<1030:RFAVTA>2.0.CO;2](https://doi.org/10.1175/1520-0485(1981)011<1030:RFAVTA>2.0.CO;2)
- Locarnini, R. A., Mishonov, A. V., Baranova, O. K., Boyer, T. P., Zweng, M. M., Garcia, H. E., et al. (2019). World Ocean Atlas 2018, Volume 1: Temperature (A. Mishonov, Technical Ed.): NOAA Atlas NESDIS.
- Lomb, N. R. (1976). Least-squares frequency analysis of unequally spaced data. *Astrophysics and Space Science*, 39, 447–462. <https://doi.org/10.1007/BF00648343>
- Luyten, J. R., & Swallow, J. C. (1976). Equatorial undercurrents. *Deep-Sea Research*, 23, 999–1001. [https://doi.org/10.1016/0011-7471\(76\)90830-5](https://doi.org/10.1016/0011-7471(76)90830-5)
- Madec, G., Bourdallé-Badie, R., Bouttier, P.-A., Bricaud, C., Bruciaferri, D., Calvert, D., et al. (2017). NEMO ocean engine. *Notes du Pôle de modélisation de l'Institut Pierre-Simon Laplace (IPSL)*, 27. <https://doi.org/10.5281/zenodo.3248739>
- Matthießen, J.-D., Greatbatch, R. J., Brandt, P., Claus, M., & Didwischus, S.-H. (2015). Influence of the equatorial deep jets on the north equatorial countercurrent. *Ocean Dynamics*, 65, 1095–1102. <https://doi.org/10.1007/s10236-015-0855-5>
- Matthießen, J.-D., Greatbatch, R. J., Claus, M., Ascani, F., & Brandt, P. (2017). The emergence of equatorial deep jets in an idealised primitive equation model: An interpretation in terms of basin modes. *Ocean Dynamics*, 67, 1511–1522. <https://doi.org/10.1007/s10236-017-1111-y>
- Ménesguen, C., Delpech, A., Marin, F., Cravatte, S., Schopp, F., & Morel, Y. (2019). Observations and mechanisms for the formation of deep equatorial and tropical circulation. *Earth and Space Science*, 6, 370–386. <https://doi.org/10.1029/2018EA000438>
- Ménesguen, C., Hua, B. L., Fruman, M. D., & Schopp, R. (2009). Dynamics of the combined extra-equatorial and equatorial deep jets in the Atlantic. *Journal of Marine Research*, 67, 323–346. <https://doi.org/10.1357/002224009789954766>
- Najjar, R. G., Sarmiento, J. L., & Toggweiler, J. R. (1992). Downward transport and fate of organic matter in the ocean: Simulations with a general circulation model. *Global Biogeochemical Cycles*, 6, 45–76. <https://doi.org/10.1029/91GB02718>
- Pacanowski, R. C., & Philander, S. G. H. (1981). Parameterization of vertical mixing in numerical models of tropical oceans. *Journal of Physical Oceanography*, 11, 1443–1451. [https://doi.org/10.1175/1520-0485\(1981\)011<1443:POVMIN>2.0.CO;2](https://doi.org/10.1175/1520-0485(1981)011<1443:POVMIN>2.0.CO;2)
- Qiu, B., Chen, S., & Sasaki, H. (2013). Generation of the north equatorial undercurrent jets by triad baroclinic Rossby wave interactions. *Journal of Physical Oceanography*, 43, 2682–2698. <https://doi.org/10.1175/JPO-D-13-099.1>
- Scargle, J. D. (1982). Studies in astronomical time series analysis. II. Statistical aspects of spectral analysis of unevenly spaced data. *The Astrophysical Journal*, 263, 835–853. <https://doi.org/10.1086/160554>
- Youngs, M. K., & Johnson, G. C. (2015). Basin-wavelength equatorial deep jet signals across three oceans. *Journal of Physical Oceanography*, 45, 2134–2148. <https://doi.org/10.1175/JPO-D-14-0181.1>
- Zweng, M. M., Reagan, J. R., Seidov, D., Boyer, T. P., Locarnini, R. A., Garcia, H. E., et al. (2019). World Ocean Atlas 2018, Volume 2: Salinity (A. Mishonov, Technical Ed.): NOAA Atlas NESDIS.